

ON THE TIDAL INTERACTION OF A SOLAR-TYPE STAR WITH AN ORBITING COMPANION: EXCITATION OF g -MODE OSCILLATION AND ORBITAL EVOLUTION

C. TERQUEM¹

UCO/Lick Observatory, University of California, Santa Cruz, CA 95064; ct@ucolick.org

J. C. B. PAPALOIZOU AND R. P. NELSON

Astronomy Unit, School of Mathematical Sciences, Queen Mary and Westfield College, University of London, Mile End Road, London E1 4NS, UK;
J.C.B.Papaloizou@qmw.ac.uk, R.P.Nelson@qmw.ac.uk

AND

D. N. C. LIN

UCO/Lick Observatory, University of California, Santa Cruz, CA 95064; lin@ucolick.org

Received 1997 September 8; accepted 1998 February 12

ABSTRACT

We calculate the dynamical tides raised on a nonrotating solar-type star by a close stellar or planetary companion. Dissipation arising from a turbulent viscosity operating in the convection zone and radiative damping in the radiative core are considered. We compute the torque exerted on the star by a companion in circular orbit and determine the potentially observable magnitude of the tidally induced velocity at the stellar photosphere. These calculations are compared to the results obtained by assuming that a very small frequency limit can be taken in order to calculate the tidal response (*equilibrium tide*). For a standard solar model the latter is found to give a relatively poor approximation at the periods of interest of several days, even when the system is far from resonance with a normal mode. This behavior is caused by the small value of the Brunt-Väisälä frequency in the interior regions of the convection zone. It is shown that although the companion may go through a succession of resonances as it spirals in under the action of the tides, for a fixed spectrum of normal modes its migration is controlled essentially by the nonresonant interaction. We find that the turbulent viscosity that is required to provide the observed circularization rates of main-sequence solar-type binaries is about 50 times larger than that simply estimated from mixing-length theory for nonrotating stars. We discuss the means by which this enhanced viscosity might be realized. These calculations are applied to 51 Pegasi. We show that the perturbed velocity induced by the tides at the stellar surface is too small to be observed. This result is insensitive to the magnitude of the turbulent viscosity assumed and is not affected by the possibility of resonance. For this system the stellar rotation and the orbital motion are expected to be synchronized if the mass of the companion is as much as $1/10 M_{\odot}$.

Subject headings: binaries: close — hydrodynamics — planetary systems — stars: interiors — stars: late-type — stars: oscillations — waves

1. INTRODUCTION

Theoretical analyses of the tidal interaction between close binaries can be classified according to whether an equilibrium tide is assumed or the dynamical tide is taken into account. The theory of the equilibrium tide is based on the assumption that a star subject to the tidal disturbance of a companion instantly adjusts to hydrostatic equilibrium (Darwin 1879). A calculation of the dynamical tide takes into account the fact that gravity or g -modes can be excited in the convectively stable layers of the star and that resonances between the tidal disturbance and the normal modes of the star can occur (Cowling 1941). So far, dynamical tides have been studied only in massive close binaries, which have a convective core and a radiative envelope (Zahn 1975, 1977; Savonije & Papaloizou 1983, 1984, 1997; Papaloizou & Savonije 1985, 1997; Savonije, Papaloizou, & Alberts 1995). In this paper we examine the effect of dynamical tides excited by a companion on a solar-type star, in which a radiative core is surrounded by a convective envelope.

This is of particular interest in connection with circularization of solar-type binaries. It has been proposed that

circularization occurs through the action of turbulent viscosity, originating in the convective envelope, on the tide. However, according to Claret & Cunha (1997; see also Goodman & Oh 1997), who have used the equilibrium tide formalism of Zahn (1989), the circularization rate resulting from this mechanism is too small by about 2 orders of magnitude to account for the circularization timescales required on the main sequence.

The tidal response calculation undertaken here is also of interest in connection with the newly discovered planets, some of which are found to orbit around solar-type stars with a period comparable to that of the high-order g -modes of the star. One such example is 51 Pegasi (Mayor & Queloz 1995; Marcy & Butler 1995).

In these binaries g -mode oscillations are excited by the companion in the radiative region beneath the convective envelope. They become evanescent in the convection zone where they are damped by their interaction with the convective eddies. Dissipation leads to an exchange of angular momentum between the star and the orbit if the stellar rotation and the orbital motion are not synchronized. Here we assume that the orbital frequency is initially larger than the rotational frequency of the star. Then, tidal interaction results in the decay of the orbit and the spin-up of the star. If the mass of the secondary companion is con-

¹ On leave from Laboratoire d'Astrophysique, Observatoire de Grenoble, Université Joseph-Fourier/CNRS, BP 53, 38041 Grenoble Cedex 9, France.

siderably smaller than that of the primary, the timescale for orbital decay is smaller than the stellar spin-up timescale, and the companion eventually plunges into the primary. But if the mass of the companion is large enough, synchronization may occur before the binary has merged, stopping further orbital decay. Estimates based on the theory of the equilibrium tide (Rasio et al. 1996; Marcy et al. 1997) suggest that the orbital decay timescale and the stellar spin-up timescale for a system like 51 Pegasi are longer than the inferred age of the primary if the companion is a Jovian-like planet.

In this paper we examine the effect of resonances on these timescales and determine the potentially observable magnitude of dynamical tides at the photosphere of a solar-type star. We also compare the dynamical tide calculations to the results of an asymptotic analysis that we carry out in the limit of small frequencies that should correspond to the adiabatic equilibrium tide theory.

The paper is organized as follows: In § 2 we study the tidal response of the star to the perturbation by a companion in a circular orbit with a period in the range 4–13 days. In § 2.1 we first consider the linear adiabatic response and then, away from resonance with a g -mode, extend the analysis using first-order perturbation theory to calculate the torque resulting from dissipation in the convective envelope. For the assumptions made about turbulent viscosity, this mechanism is then found to be more important than nonadiabaticity arising from heat transport in the radiative interior (i.e., radiative damping). However, this is not the case in the vicinity of a g -mode resonance. There we also calculate the torque caused by nonadiabaticity in the radiative core using a WKB treatment of the nonadiabatic terms. We find that the torque at effective resonances is mainly determined by radiative damping. An analysis valid for very low frequencies (*equilibrium tide*) is given in § 2.2.

The orbital circularization timescale for systems initially in noncircular orbits can be derived from the response calculations for companions in circular orbits. This is done in § 2.3. We then discuss how this might be used to calibrate the magnitude of the turbulent viscosity required to fit the observations in § 2.4.

Numerical calculations are presented in § 3. The results assuming the equilibrium tide are given in § 3.1. In § 3.2 we present the results of the dynamical tide calculations. We describe the tidal response of the star to a companion in circular orbit, give the induced velocity at its surface, and the tidal torque. We describe the resonances and show that, for the periods of interest of several days, they are not expected to affect the orbital evolution of the binary. In § 3.3 we compare the calculations based on the dynamical and equilibrium tides. We find that for the standard solar model at the orbital periods of interest, because of the long timescale associated with convection, the equilibrium tide calculations give a relatively poor approximation to the results of the dynamical tide calculations.²

We find that the viscosity that is required to provide the observed circularization rates is about 50 times larger than that simply estimated from mixing-length theory and discuss the means by which this viscosity might be enhanced in § 3.4. However, we note that *the strength of the resonances for orbital periods larger than ~8 days and the*

perturbed velocity at the surface of the star are insensitive to the magnitude of the turbulent viscosity assumed. Only for periods ~4 days is the strength of the resonances decreased by a factor ~4. The observable width of the resonances is also reduced when the viscosity is increased. We also give the relation between the orbital evolution, circularization, and spin-up timescales and the orbital frequency in § 3.5.

Finally in § 4 we discuss and summarize our results, applying them to 51 Pegasi in § 4.1.

2. TIDAL RESPONSE TO A COMPANION IN CIRCULAR ORBIT

The calculations presented in this section will be applied to close binary systems where the primary is a solar-type star and the secondary is a stellar or planetary companion. The orbital periods of interest lie in the range 4–13 days. The rotational angular velocity of the primary is assumed to be small compared to the orbital frequency, so that it can be neglected. Quadrupolar tidal forcing thus occurs through potential perturbations with periods in the range 2–6.5 days.

When calculating the tidal response well away from a condition of resonance with a g -mode, we first calculate the tidal response assuming it to be adiabatic throughout the star. First-order perturbation theory is then used to calculate the dissipation occurring in the convective envelope. The idea here (as is borne out by the numerical results) is that although short-wavelength g -modes are excited in the radiative core, when they are away from resonance they do not play an important role in comparison with the global component of the tidal response for large enough turbulent viscosity. Also, the variations in the convective envelope occur on a comparatively long length scale, making the adiabatic approximation a reasonable one.

When there is a resonance with a high-order g -mode, the response becomes one with a very short length scale, such that nonadiabaticity in the radiative core cannot be neglected. However, the modes are of high order, such that a WKB treatment of the nonadiabatic effects is possible, and this is used close to resonance where the normal mode dominates the response. Such nonadiabatic effects turn out to be more important than the action of turbulent viscosity in the convective envelope, with the torque at significant resonances being determined mainly by nonadiabatic effects.

2.1. Linearized Equations

2.1.1. Adiabatic Perturbations

The linearized momentum, mass, and energy equations governing the adiabatic response of the nonrotating star to the perturbing potential Ψ_T may be written as (see, e.g., Unno et al. 1989)

$$\frac{\partial^2 \xi}{\partial t^2} = -\frac{1}{\rho} \nabla P' + \frac{\rho'}{\rho^2} \nabla P - \nabla \Psi_T, \quad (1)$$

$$\rho' = -\nabla \cdot (\rho \xi), \quad (2)$$

$$\Delta S = 0, \quad (3)$$

where P is the pressure, ρ is the density, S is the entropy, ξ is the Lagrangian displacement vector, Δ denotes the Lagrangian perturbation, and the primed quantities are Eulerian perturbations. We use the Cowling (1941) approximation, applicable to stars with high central condensation,

² By dynamical tide we mean the full tidal response calculated without the assumption of hydrostatic equilibrium.

which neglects the perturbation to the stellar gravitational potential. We also have the thermodynamic relation

$$\Delta S = \frac{P}{\rho T} \frac{1}{\Gamma_3 - 1} \left(\frac{\Delta P}{P} - \Gamma_1 \frac{\Delta \rho}{\rho} \right), \quad (4)$$

where T is the temperature, and Γ_1 and Γ_3 are the adiabatic exponents of Chandrasekhar. This relation, together with equation (3), leads to

$$\frac{\rho'}{\rho} = \frac{P'}{\Gamma_1 P} - A \xi_r, \quad (5)$$

where

$$A = \frac{d \ln \rho}{dr} - \frac{1}{\Gamma_1} \frac{d \ln P}{dr} = -\frac{N^2}{g}, \quad (6)$$

with $\text{sgn}(N^2)|N^2|^{1/2}$ being the Brunt-Väisälä frequency, and g being the acceleration due to gravity.

Following Cowling (1941), only the dominant quadrupole term is considered in the perturbing potential arising from the companion. For a binary system with a circular orbit, this is given in spherical polar coordinates (r, θ, φ) by the real part of

$$\Psi_T(r, \theta, \varphi, t) = fr^2 Y_{n,m}(\theta, \varphi) e^{-im\omega t}, \quad (7)$$

where the spherical harmonic

$$Y_{n,m}(\theta, \varphi) = P_n^{|m|}(\cos \theta) e^{im\varphi},$$

with $n = m = 2$, $P_n^{|m|}$ being the associated Legendre polynomial with indices n and m . Here ω is the orbital angular velocity; $f = -GM_p/4D^3$, where D is the orbital separation; and M_p is the mass of the companion. We adopt the same angular and time dependence for the perturbations, so that P' , ρ' , and S' are proportional to $Y_{n,m}(\theta, \varphi) \exp(-im\omega t)$. The corresponding expression for the Lagrangian displacement is

$$\xi = \left[\xi_r(r), \xi_h(r) \frac{\partial}{\partial \theta}, \xi_h(r) \frac{\partial}{\sin \theta \partial \varphi} \right] Y_{n,m}(\theta, \varphi) e^{-im\omega t}. \quad (8)$$

The factor $Y_{n,m}(\theta, \varphi) \exp(-im\omega t)$ will be henceforth taken as read, so that hereafter the perturbations will be taken to depend only on r . Physical perturbations are then found by taking real parts after inserting this factor.

The horizontal displacement ξ_h is given by the nonradial equation of motion (1):

$$\xi_h = \frac{1}{m^2 \omega^2 r} \left(\frac{P'}{\rho} + fr^2 \right). \quad (9)$$

This relation, together with equation (5), allows P' and ρ' to be eliminated from the system of equations (1)–(3). The radial equation of motion (1) and the continuity equation (2) can then be written as a pair of ordinary differential equations for ξ_r and ξ_h :

$$\begin{aligned} \frac{d\xi_r}{dr} = & \left(-\frac{2}{r} + A - \frac{d \ln \rho}{dr} \right) \xi_r \\ & + \left[-\frac{m^2 \omega^2 r \rho}{\Gamma_1 P} + \frac{n(n+1)}{r} \right] \xi_h + \frac{fr^2 \rho}{\Gamma_1 P}, \end{aligned} \quad (10)$$

$$\frac{d\xi_h}{dr} = \frac{1}{r} \left(1 - \frac{AP}{m^2 \omega^2 \rho} \frac{d \ln P}{dr} \right) \xi_r - \left(A + \frac{1}{r} \right) \xi_h + \frac{Afr}{m^2 \omega^2}, \quad (11)$$

the solution of which requires two boundary conditions. At the surface of the star we take a free boundary: $\Delta P = 0$, i.e., $P' = -\xi_r dP/dr$. The boundary condition at $r = 0$, where equations (10) and (11) have a regular singularity, is that the solutions be regular. Since at $r \sim 0$, $P = P_c + O(r^2)$, $\rho = \rho_c + O(r^2)$, and $A = O(r)$, where P_c and ρ_c are, respectively, the central pressure and density, this leads to $\xi_h = \xi_r/n$.

2.1.2. Torque Caused by Dissipation in the Convective Envelope

The interaction between convective motions and the tidal flow is expected to lead to the dissipation of tidally excited waves (e.g., Zahn 1977). We model this effect as arising from a turbulent viscosity. To do this we suppose there is an additional dissipative force per unit mass acting in the convection zone, given in spherical coordinates by

$$F_c = \frac{1}{\rho r^2} \frac{\partial}{\partial r} \left(\rho r^2 \nu \frac{\partial v}{\partial r} \right), \quad (12)$$

where v is the flow velocity, and ν is the turbulent viscosity. Here, we assume that variation in the radial direction is the most significant and note that the viscous force is defined in such a way as to lead to a positive-definite energy dissipation rate.

For the turbulent viscosity coefficient we take (see, e.g., Xiong, Cheng, & Deng 1997)

$$\nu = \frac{c_1}{t_c} \frac{\Lambda^2}{1 + c_2 (m t_c / P_o)^s}, \quad (13)$$

where c_1 and c_2 are two constants, c_1 being on the order of unity, $P_o = 2\pi/\omega$ is the orbital period, Λ is the mixing length, and $t_c = 1/|N^2|^{1/2}$ is the convective timescale. The viscosity is then $c_1 \Lambda^2/t_c$ for small forcing frequency $m\omega$. The factor $1 + c_2 (m t_c / P_o)^s$, where we shall use $s = 2$, allows for a reduction of efficiency of the damping of high-frequency oscillations to which the convection cannot adjust. A similar prescription with $s = 1$ has been proposed by Zahn (1966) and used by Zahn (1989), whereas $s = 2$ has been considered by Goldreich & Keeley (1977) and used by Campbell & Papaloizou (1983) and Goldman & Mazeh (1991). Goodman & Oh (1997) have also recently put forward some arguments in favor of $s = 2$. For the mixing length we shall take the standard relation $\Lambda = \alpha/|d \ln P/dr|$ and set $\alpha = 3$.

In principle, equations (1)–(3) should be solved with F_c added on the right-hand side of equation (1) in the convective envelope. However, this would increase the order of the differential system to be solved and make the numerical calculations much more complicated. Instead, we have found it adequate to solve first the adiabatic problem and then to treat the dissipative effect using a first-order perturbation theory. This is valid everywhere, except very close to resonances, because dissipation is weak enough so that the imaginary parts of ξ_r and ξ_h are much smaller in magnitude than their real parts. Thus, we solve equations (1)–(3) without dissipative terms and use these (real) solutions to calculate the rate of energy dissipation dE/dt arising from convection, given by

$$\frac{dE}{dt} = - \int_{V_c} \rho \text{Re}(F_c) \cdot \text{Re}(v) dV, \quad (14)$$

where the integration is over the volume V_c of the convective envelope, and the angular dependence of F_c and v has to be taken into account. Using the relation $v = \partial \xi / \partial t$ and

the expression (8) for ξ , we obtain

$$\frac{dE}{dt} = -\frac{48\pi}{5} m^2 \omega^2 \int_{R_i}^{R_c} \rho r^2 v \left[\left(\frac{\partial \xi_r}{\partial r} \right)^2 + 6 \left(\frac{\partial \xi_h}{\partial r} \right)^2 \right] dr, \quad (15)$$

where R_i and R_c are, respectively, the inner and outer radii of the convective envelope. Noting that the ratio of the rate of exchange of energy and angular momentum with the orbit is given by the pattern speed of the tidal disturbance ω , the torque exerted by the companion on the star is given by

$$\mathcal{T} = -\frac{1}{\omega} \frac{dE}{dt}. \quad (16)$$

This torque is positive because the star is nonrotating.

When the frequency of the tidal wave is equal to that of some adiabatic normal-mode frequency of the star, we can no longer use first-order perturbation theory, because it would give an infinite torque. However, when the frequency ω is very close to a resonant frequency ω_0 , the torque will be given by an expression of the form

$$\mathcal{T} = \frac{\mathcal{A}}{m^2(\omega - \omega_0)^2 + \gamma^2}, \quad (17)$$

where \mathcal{A} is an amplitude, and γ is the damping rate for the mode. First-order perturbation theory assumes that dissipative effects are small in the response calculation. Therefore, it is valid only for frequencies such that $m^2(\omega - \omega_0)^2 \gg \gamma^2$. However, the damping rate, if small, can be found from first-order perturbation theory, applied, as described above, very close to resonance where the mode dominates the response. Then, it is given by (see, e.g., Goldstein 1980)

$$2\gamma = -\frac{1}{2E_K} \frac{dE}{dt}, \quad (18)$$

very close to resonance, where E_K is the kinetic energy of the mode,

$$E_K = \frac{1}{2} \int_V \rho [\text{Re}(v)]^2 dV = \frac{24\pi}{5} m^2 \omega^2 \int_0^{R_\odot} \rho r^2 (\xi_r^2 + 6\xi_h^2) dr, \quad (19)$$

the integration being over the volume V of the star. (In the first integral the angular dependence of v has to be taken into account.) In equation (18) the total energy of the mode is $2E_K$, because at resonance there is equipartition between kinetic and potential energy. We calculate γ using equation (18) as outlined above, making sure that ω is close enough to ω_0 by checking that γ remains approximately constant when ω is slightly changed. To get \mathcal{A} we fit the torque obtained from first-order perturbation theory to equation (17) in the region approaching the resonance, where $m^2(\omega - \omega_0)^2 \gg \gamma^2$ still. This procedure works satisfactorily when γ is small, with consequent strong resonances. This appears to be the situation when turbulent viscosity alone is assumed to act. However, radiative damping cannot be neglected for resonances at low forcing frequency; this is discussed below.

2.1.3. Torque Caused by Nonadiabaticity in the Radiative Core

Nonadiabatic effects become important when the radiative diffusion time across the length scale associated with

the tidal response shortens to become comparable to the wave propagation time across the star. In principle these effects should be taken into account both in the radiative core and above the convection zone. However, since g -modes, which are excited in the radiative core, are evanescent in the convective envelope, we do not expect non-adiabaticity to play an important role above the convection zone. To take nonadiabatic effects into account, equation (3) has to be modified in the radiative core to

$$\rho T \frac{\partial(\Delta S)}{\partial t} = -\nabla \cdot \mathbf{F}', \quad (20)$$

where \mathbf{F}' is the perturbed radiative flux. Here for simplicity we neglect gradients in the chemical composition. The radiative flux is given by the radiative diffusion equation

$$\mathbf{F} = -K\nabla T,$$

where T is the temperature, and $K = 4acT^3/(3\kappa\rho)$ is the radiative conductivity, with a being the Stefan-Boltzmann radiation constant, c being the velocity of light, and κ being the opacity. Therefore,

$$\nabla \cdot \mathbf{F}' = -\frac{1}{r^2} \frac{\partial}{\partial r} \left[r^2 \left(K \frac{\partial T'}{\partial r} + K' \frac{dT'}{dr} \right) \right] - \nabla_h^2(KT'), \quad (21)$$

where ∇_h is the nonradial component of the operator ∇ . We now suppose that close to resonance, the response behaves exactly like a free g -mode with very large radial wavenumber k_r , so that WKB theory can be used together with the local dispersion relation to evaluate $\nabla \cdot \mathbf{F}'$. The dominant term in the right-hand side of equation (21) is then $-K \partial^2 T' / \partial r^2 = K k_r^2 T'$, and all the other terms can be neglected. For a high-order free g -mode, the local dispersion relation gives (see, e.g., Unno et al. 1989)

$$k_r^2 = \frac{N^2}{(m\omega)^2} \frac{n(n+1)}{r^2}. \quad (22)$$

This expression of k_r is derived under the adiabatic approximation. However, since we want to incorporate non-adiabatic effects to the lowest order, we do not need to take them into account in evaluating k_r . We have $k_r \gg 1/r$ in the radiative core because $N \gg m\omega$ there. The perturbed temperature T' can be expressed as a function of P' and ρ' using the thermodynamic relation

$$\frac{T'}{T} = \frac{1}{\chi_T} \frac{P'}{P} - \frac{\chi_\rho}{\chi_T} \frac{\rho'}{\rho}, \quad (23)$$

where $\chi_T = \partial \ln P / \partial \ln T|_\rho$, and $\chi_\rho = \partial \ln P / \partial \ln \rho|_T$.

The equation of state in the radiative core of a solar-type star is primarily that of a perfect gas (we neglect here the radiation pressure, which is very small compared to the gas pressure). We then have $\Gamma_1 = \Gamma_3 = 5/3$ and $\chi_\rho = \chi_T = 1$. Using the above, the facts that $n = 2$ and $\partial/\partial t = -im\omega$, and equation (4), we can recast equation (20) in the form

$$\frac{\rho'}{\rho} = \frac{1 + i\epsilon\Gamma_1}{1 + i\epsilon} \frac{P'}{\Gamma_1 P} - \frac{A}{1 + i\epsilon} \xi_r, \quad (24)$$

where

$$\epsilon = \frac{16acT^4 N^2}{5(m\omega)^3 \kappa \rho P r^2}. \quad (25)$$

For high-order free g -modes, we have (see, e.g., Unno et al. 1989)

$$\frac{P'/P}{A\xi_r} \sim \frac{m\omega}{N} \frac{d \ln P}{d \ln r},$$

which means that $|P'/P| \ll |A\xi_r|$ in the radiative core of a solar-type star at the frequencies of interest. The non-adiabatic correction of the term associated with pressure in equation (24) is then very small compared to the non-adiabatic correction of the term involving ξ_r . Therefore, equation (24) can be approximated by

$$\frac{\rho'}{\rho} = \frac{P'}{\Gamma_1 P} - \bar{A}\xi_r, \quad (26)$$

where we have defined $\bar{A} = A/(1 + i\epsilon)$. We note that because we have identified the tidal response with a normal mode, this calculation is valid only close to resonances. Equation (26) is similar to equation (5), but with A being replaced by \bar{A} . The system of differential equations that we have to solve to get the nonadiabatic response of the star is then the same as equations (10) and (11), but with the following modification in the radiative core. In equations (10) and (11), A , where it appears as a coefficient of ξ_r , has to be replaced by \bar{A} . The system of differential equations so obtained is complex. In general, for the periods that we consider, $\epsilon \leq 5 \times 10^{-4}$ is small. We then calculate both the real and imaginary parts of the response, so that the torque can be computed directly from

$$\mathcal{T} = - \int_V \rho' \frac{\partial \Psi_T}{\partial \varphi} dV, \quad (27)$$

where the integral is over the volume V of the star. The angular dependence of Ψ_T and ρ' has to be taken into account in this expression. Equation (27) can be recast in the form (Savonije & Papaloizou 1983)

$$\mathcal{T} = - \frac{96\pi f}{5} \int_0^{R_\odot} \text{Im}(\rho') r^4 dr. \quad (28)$$

As in § 2.1.2, we can calculate the damping rate γ' in resonances resulting from nonadiabatic effects using equation (18). Here, the rate of energy dissipation is calculated from the torque (see eq. [16]).

2.2. Low-Frequency Limit

In the limit of small ω , the following relations may be obtained for the *adiabatic equilibrium tide*:

$$P'_{\text{eq}} = -fr^2\rho, \quad (29)$$

and, if $N^2 \neq 0$:

$$\xi_{r,\text{eq}} = fr^2\rho \left(\frac{dP}{dr} \right)^{-1}, \quad (30)$$

$$\xi_{h,\text{eq}} = \frac{1}{n(n+1)r} \frac{d}{dr} (r^2 \xi_{r,\text{eq}}), \quad (31)$$

where the subscript “eq” denotes the equilibrium value. Using these displacements, the torque may be calculated using equations (15) and (16).

However, we comment that equation (30), which states that the Lagrangian perturbation to the pressure is zero, can only be derived in the adiabatic low- ω limit if the

Brunt-Väisälä frequency is not zero (in practice, one also requires that the forcing period be short compared to the thermal timescale of the star, but the latter is so long that it can be assumed to be infinite in this context). Equations (30) and (31) do not apply in a finite region where strictly $N^2 = 0$. In that case the fluid is locally barotropic, and the displacement can be written as the gradient of a potential:

$$\xi = \nabla[\Phi(r)Y_{n,m}]. \quad (32)$$

The continuity equation then gives, for low frequencies,

$$\begin{aligned} \nabla \cdot (\rho\xi) &= \frac{1}{r^2} \frac{d}{dr} \left(r^2 \rho \frac{d\Phi}{dr} \right) - \frac{n(n+1)\rho\Phi}{r^2} \\ &= -\rho'_{\text{eq}} = -\frac{P'_{\text{eq}}\rho}{\Gamma_1 P} = \frac{fr^2\rho^2}{\Gamma_1 P}. \end{aligned} \quad (33)$$

Equation (33) gives a second-order differential equation for $\Phi(r)$. This applies inside the region where $N^2 = 0$. It is possible, using the two available boundary conditions for equation (33), to match $\xi_{r,\text{eq}}$ given by equation (30) at the boundaries of such a region, but not in general $\xi_{h,\text{eq}}$ given by equation (31). This means that there will tend to be a discontinuity in the tangential displacement at the boundaries for low frequencies.

When $|N^2|$ is not zero, but very small, in particular small compared to $m^2\omega^2$, which corresponds physically to the convective timescale being much longer than the forcing period, the tidal response more closely matches that given by equation (33) than that given by equations (30) and (31). This feature causes a very slow convergence toward the low-frequency limiting solution (*equilibrium tide*) found here, as well as near discontinuous behavior near the inner convective envelope boundary. This is borne out by our numerical results (see §§ 3.2.1 and 3.3).

2.3. Timescales

2.3.1. Orbital Evolution and Stellar Spin-up Timescales

The torque \mathcal{T} gives the rate at which angular momentum is transferred from the orbit to the star. We can then calculate a tidal evolution (decay) timescale of the circular orbit:

$$t_{\text{orb}} = \frac{\mu\omega D^2}{\mathcal{T}}, \quad (34)$$

where $\mu = M_p M_\odot / (M_p + M_\odot)$ is the reduced mass. In principle, the variation of the torque with ω has to be taken into account for the total decay time to be calculated. However, since the torque increases as the companion spirals in, t_{orb} is mainly determined by the initial position of the companion, and a good estimate can be obtained by using the above formula.

This exchange of angular momentum also results in the spin-up of the star, the timescale of which is given by $t_{\text{sp}} = I\omega/\mathcal{T}$ (Savonije & Papaloizou 1983), with I being the stellar moment of inertia. Out of resonance, angular momentum deposition *initially* occurs mainly in the convective envelope where the turbulent viscosity acts (Goldreich & Nicholson 1989). It is then of interest to calculate the spin-up timescale for the convective envelope alone, which is $t_{\text{sp},c} = I_c \omega / \mathcal{T}$, where I_c is the moment of inertia of the convection zone. We note, however, that on the long timescales associated with tidal evolution, angular momentum may be redistributed throughout the star.

2.3.2. Circularization

In practice we find that the torque caused by turbulent viscosity acting on the tide arising from a companion in a circular orbit varies with frequency approximately $\propto \omega^4$. This result can be used to relate the orbital circularization timescale to the initial orbital decay timescale, provided that the eccentricity is not too large. In practice, both these timescales can be significantly longer than the spin-up timescale of the star, because of its relatively small moment of inertia. We should then consider that the star is synchronized with the orbit.

The ratio between the orbital decay timescale and the circularization timescale t_{circ} is found to be about 6 for the calculated frequency dependence of the circular orbit torque (see, e.g., the expressions given in Savonije & Papaloizou 1983, 1984). This appears to be independent of whether the star is assumed to be synchronously rotating or nonrotating, in that the circularization rate calculated assuming no rotation, as we do here, gives a reasonable estimate in the synchronous case also.³ In addition, to evaluate t_{circ} for an equal-mass system, we have to take into account the reciprocal torque exerted by the primary on the companion. To do this we take t_{circ} to be proportional to a factor that is $\frac{1}{2}$ when $M_p = M_\odot$ and is 1 when $M_p \ll M_\odot$. To a reasonable approximation, we then obtain

$$t_{\text{circ}} = \frac{t_{\text{orb}}}{6(1 + M_p/M_\odot)}. \quad (35)$$

2.4. Circularization Timescale as a Calibration of Turbulent Viscosity

One of the purposes of this paper is to calculate the tidally induced velocities on the star. In order to do this the processes responsible for dissipating the disturbance should be included as accurately as possible. An important dissipation process is that associated with turbulent friction in the convection zone. As this process has been suggested as being responsible for circularizing the orbits of main-sequence binaries of sufficiently short period (see Mathieu 1994), we investigate whether reasonable assumptions about the behavior of turbulent viscosity can lead to the observed circularization rates.

2.4.1. Background

Zahn & Bouchet (1989) have investigated the pre-main-sequence evolution of late-type binaries in which the stars are fully convective. The main conclusion of their work was that circularization occurs at the very beginning of the Hayashi phase, with hardly any decrease of the eccentricity on the main sequence. The cutoff period they predict is between 7.3 and 8.5 days. According to them, observations show a cutoff period around 8 days, independent of the age of the star, and are then in agreement with their results.

However, we note that for this agreement to be reached, some observations had to be discarded. Those by Mayor & Mermilliod (1984), which indicated that the cutoff period of late-type binaries was at most 5.7 days, and those by Mathieu & Mazeh (1988), which showed that the cutoff period in the 4 Gyr old cluster M67 was more than 10 days. In a review article Mathieu (1994; see also Mathieu 1992

and Mathieu et al. 1992) has confirmed that “cutoff periods increase with age, consistent with active main-sequence tidal circularization.” The pre-main-sequence cutoff period is very likely to be 4.3 days (an upper limit being 6.4 days), and cutoff periods for solar-mass binaries are 7.05 days in the Pleiades (0.1 Gyr), 8.5 days in the Hyades (0.8 Gyr), 12.4 days in M67 (4 Gyr), and 18.7 days in the halo field (16 Gyr). It is then reasonable to conclude that active circularization does take place for main-sequence binaries and that it is less efficient than proposed by Zahn & Bouchet (1989) on the pre-main-sequence.

Recently Claret & Cunha (1997) have applied the formalism developed by Zahn (1989) to different stellar models. They have computed the parameters that enter into the expression for the circularization timescale, which is based on treatment of the equilibrium tide, for a wide grid of stellar models as a function of mass and time. Their conclusion is that turbulent dissipation is too low by a factor of 100–200 during the main sequence to fit the observed cutoff periods.

3. NUMERICAL RESULTS

The calculations presented in the § 3.1 are applied to the standard solar model described by Christensen-Dalsgaard et al. (1996).

3.1. Equilibrium Tide

The torque associated with the equilibrium tide was calculated as indicated in § 2.2. As mentioned there, this calculation is only expected to apply at very low frequencies. For periods between 4.23 and 12.4 days, and $c_1 = c_2 = 1$, the calculated torque can be interpolated by the following power law:

$$\mathcal{T}(\text{g cm}^2 \text{ s}^{-2}) = 1.200 \times 10^{55} \left(\frac{M_p}{M_p + M_\odot} \right)^2 \omega^{4.08}. \quad (36)$$

3.2. Dynamical Tide

For the calculation of the dynamical tide, we solve the differential equations (10) and (11) numerically using a shooting method to an intermediate fitting point (Press et al. 1986). To evaluate nonadiabatic effects in the radiative core close to resonances, we modify these equations as described in § 2.1.3. We define the dimensionless quantity $x \equiv r/R_c$, where R_c is the outer radius of the convective envelope. With this notation, the equations are integrated from $x_{\text{in}} = 10^{-6}$ to $x_{\text{out}} = 1.00071256$. The radiative core extends from $x = 0$ to $x \simeq 0.7$. The results presented below have been obtained with the values $c_1 = c_2 = 1$ and $\alpha = 3$ (α being the ratio of the mixing length Λ to the pressure scale height). We discuss the effect of changing these parameters.

3.2.1. Tidal Response and Velocity at the Surface of the Star

For illustration purposes, we plot the horizontal and radial displacements induced in the star at orbital periods of $P_o = 4.23$ and 8.46 days away from resonance in the adiabatic approximation. The first period is that inferred for the system 51 Pegasi. The spatial distribution of the real parts of $m\omega\xi_r$ and $m\omega\xi_h$ are shown in Figure 1. These represent typical values of the radial and horizontal velocities, the maximum values being 3 and 6 times larger, respectively. Since these quantities depend on the perturbing mass through the ratio $M_p/(M_p + M_\odot)$, they have been represented in units of this factor.

³ Note that the effects of g -mode resonances are not included in these estimates.

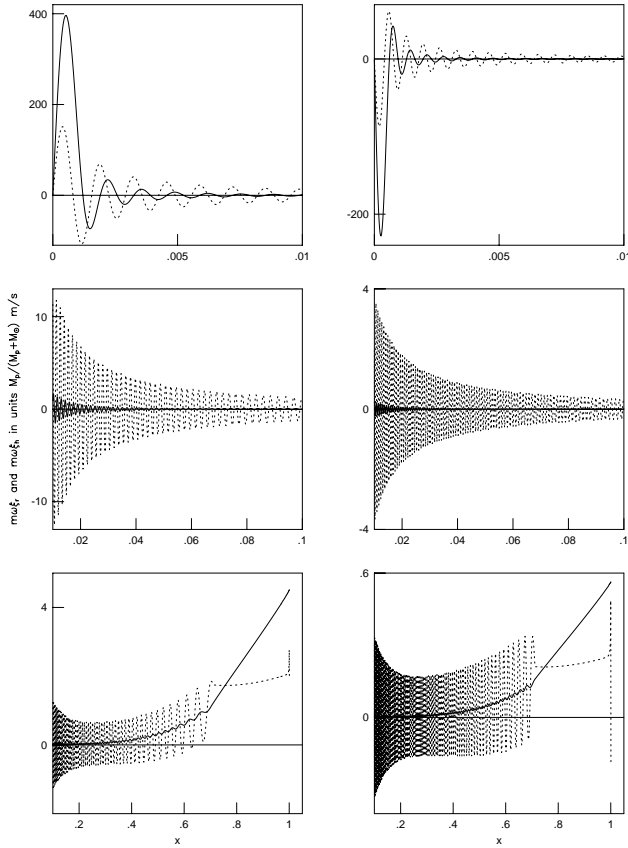


FIG. 1.—Real part of $m\omega\xi_r$ (solid lines) and $m\omega\xi_h$ (dotted lines) in units of $M_p/(M_p + M_\odot)$ m s⁻¹ vs. x for $x_{in} \leq x \leq 0.01$ (top), $0.01 \leq x \leq 0.1$ (middle), and $0.1 \leq x \leq x_{out}$ (bottom) and for $P_o = 4.23$ (left) and 8.46 (right) days. These represent typical values of the radial and horizontal velocities, the maximum values being 3 and 6 times larger, respectively.

As expected, the stellar response shows oscillations between turning points near the center and the inner radius of the convection zone, where $m^2\omega^2 = N^2$; otherwise it is evanescent. The horizontal displacement varies rapidly in the photosphere because the temperature drops to zero rapidly there.

We see from Figure 1 that when the perturbing mass $M_p = M_\odot$, the maximum radial velocity at the surface of the star is about 6 and 1 m s⁻¹ for $P_o = 4.23$ and 8.46 days, respectively. These numbers drop to 10^{-2} and 2×10^{-3} , respectively, when the perturbing mass is 1 Jupiter mass ($M_p = 10^{-3} M_\odot$).

The radial displacement and the perturbed pressure at the surface of the star are well approximated by the equilibrium values, equations (30) and (29), respectively. These quantities are found to be insensitive to the existence of resonances calculated taking nonadiabatic effects into account, with the consequence that the radial velocity at the surface of the star never differs much from the values given above. For the smallest periods considered, the ratio $|\text{Re}(\xi_h)/\text{Re}(\xi_r)|$ at the surface of the star can vary by up to 1 order of magnitude on passage through resonance. This results from the fact that ξ_h is proportional to $(P' - P'_{eq})/P$ (see eq. [9]). Even though this ratio remains small, it can vary by up to an order of magnitude as a resonance is passed through.

The numerical results indicate that both the amplitude and the wavelength of the response increase with the orbital

frequency, in agreement with the theoretical expectation of a smaller radial order for higher frequencies (Christensen-Dalsgaard & Berthomieu 1991 and references therein).

Finally, as expected (see § 2.2), the plots shown in Figure 1 (see also Fig. 3) indicate that at the boundary of the radiative core and the convection zone, there is a near discontinuity in the mean value of ξ_h obtained after averaging out the interior oscillations.

3.2.2. Circular Orbit Torque

3.2.2.1. Resonances

Figure 2 shows \mathcal{T} versus ω in a log-log representation for three different small frequency intervals in the vicinity of $P_o = 4.23, 8.5,$ and 12.4 days. On each plot the dotted line gives the values obtained from the theory of the equilibrium tide as given by equation (36). Since the torque depends on the perturbing mass through the factor $M_p^2/(M_p + M_\odot)^2$, it has been represented in units of the latter. These plots show several resonances, which occur when the frequency of the tidal wave is equal to the frequency of some normal mode of the star. The left panels show the torque arising from convective dissipation, through turbulent viscosity, alone (see § 2.1.2). These plots have been displayed for comparison with the right panels, for which radiative damping has been taken into account in the resonances (see § 2.1.3).

As indicated by the Table 1 the normal-mode damping rate owing to radiative damping (γ') is much larger than that due to convective dissipation (γ). Thus, the torque in

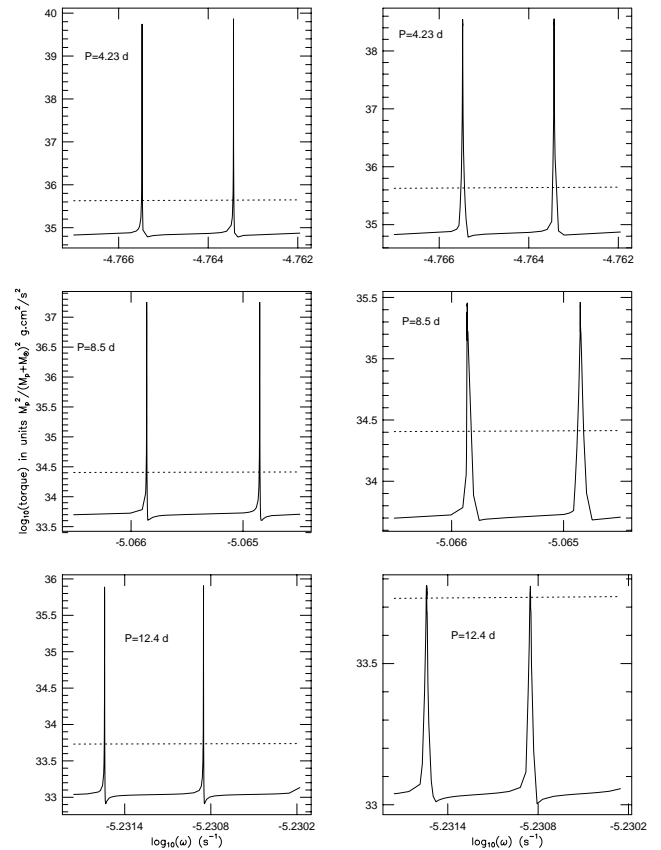


FIG. 2.—Shown is $\log_{10} \mathcal{T}$ with \mathcal{T} in units of $M_p^2/(M_p + M_\odot)^2$ g cm² s⁻² vs. $\log_{10} \omega$ for $P_o = 4.23$ (top), 8.5 (middle), and 12.4 (bottom) days. The solid and dotted lines correspond, respectively, to the dynamical and equilibrium tides calculations. Left: \mathcal{T} is calculated using convective dissipation only. Right: \mathcal{T} is calculated using radiative dissipation alone in the resonances and convective dissipation alone away from resonances.

TABLE 1
NORMAL-MODE DAMPING RATES

P_o (days)	ω (s^{-1})	γ (s^{-1})	γ' (s^{-1})
4.23.....	1.72×10^{-5}	6×10^{-12}	10^{-10}
8.5.....	8.56×10^{-6}	5×10^{-12}	7×10^{-10}
12.4.....	5.86×10^{-6}	4×10^{-12}	2×10^{-9}

the center of resonances, where they are significant, is predominantly determined by radiative damping. For the frequencies that we consider and $c_2 = 1$, this contribution to the torque becomes much smaller than that from turbulent viscosity in the tail of the resonances. This means that non-adiabatic effects in the radiative core are negligible away from resonances. Therefore, in the right panels of Figure 2 we have plotted the torque resulting from radiative damping acting alone in the center of resonances and that resulting from convective dissipation acting alone away from resonances. A comparison between the strength of the resonances shown in the right and left panels indicates the importance of nonadiabatic effects in the radiative core. As expected, the resonances are weakened and broadened, this effect being marginally important for $P_o \sim 4.23$ days.

We now discuss the properties and the effect of resonances on the tidal torque. From now on, when resonances are discussed, we shall refer to the calculations that take into account radiative damping.

In the neighborhood of $P_o = 4.23, 8.5,$ and 12.4 days, the relative separation $\Delta\omega/\omega$ between successive resonances is, respectively, $4.5 \times 10^{-3}, 2 \times 10^{-3},$ and 10^{-3} . The relative width $\delta\omega/\omega$ of the resonances is, respectively, $3 \times 10^{-4}, 1.5 \times 10^{-4},$ and 10^{-4} . Here we have arbitrarily defined the width of a resonance as being the frequency interval over which \mathcal{T} is at least 3 times larger than the minimum torque obtained just out of this resonance. From these widths we can also extrapolate the torque due to radiative damping midway between resonances using equation (17) remembering to take account of the resonances on either side. Then we find the torques midway between resonances to be factors of 37, 30, and 17 below the torques due to turbulent viscosity with $c_2 = 1$ at periods of 4.23, 8.5, and 12.4 days, respectively.

To calculate the probability of the companion being in a resonance, we have to take into account the fact that it drifts away from the resonances much more rapidly than elsewhere. The relevant quantity for calculating the tidal evolution timescale is $1/\mathcal{T}$ (see eq. [34]). For a fixed oscillation spectrum, we can approximate this probability by $\delta\omega/\Delta\omega$ times the ratio of the mean value of $1/\mathcal{T}$ over a resonance to the mean value of $1/\mathcal{T}$ between two resonances, where the mean value is defined by

$$\left\langle \frac{1}{\mathcal{T}} \right\rangle = \int \frac{d\omega}{\mathcal{T}} / \int d\omega,$$

with the integrals being taken over the relevant frequency interval.

This gives a probability of being in a resonance that is close to 0.7% for $P_o = 4.23$ and 8.5 days and 2% for $P_o = 12.4$ days. The fact that the probability of being in a resonance increases with P_o is not significant, because resonances get weaker when the period increases (see Fig. 2).

We note that this discussion applies only if the a priori probability of being in any frequency interval of a given width is independent of the frequency, as might be expected to be a reasonable assumption if the normal-mode spectrum is fixed. However, different circumstances may apply if the combined effect of orbital and stellar evolution were to lock the companion in a resonance with changing location. But we shall not consider the possibility of this process here.

As the companion spirals inward, it goes through a succession of resonances. However, for a fixed normal-mode spectrum, the above calculation tells us that its migration is controlled essentially by the nonresonant interaction. This can be seen by comparing $\langle 1/\mathcal{T} \rangle$ evaluated over a large frequency range, both taking into account and neglecting the resonances. Such a comparison shows that neglecting resonances changes $\langle 1/\mathcal{T} \rangle$ by at most a few percent.

3.2.2.2. Relation between the Mean Torque, ω , and the Circularization Timescale

Here we interpolate the numerical results to express the torque as a power of the frequency. To begin with, we consider the three frequency intervals described above. We take the appropriate torque to be $1/\langle 1/\mathcal{T} \rangle$, where the mean values are taken over the frequency intervals displayed in Figure 2. The results can be interpolated with the following relation:

$$\mathcal{T} (\text{g cm}^2 \text{ s}^{-2}) = 1.654 \times 10^{53} \left(\frac{M_p}{M_p + M_\odot} \right)^2 \omega^{3.85}. \quad (37)$$

We have checked that the above formula gives a good estimate of the torque at other nonresonant frequencies between 4.23 and 12.4 days. Since the index of the power law equation (37) is close to 4, the circularization timescale t_{circ} is given by equation (35). At $P_o = 12.4$ days, t_{circ} is found from the above formula to be 56 times larger than the timescale of 4 Gyr that is indicated by the observations.

We note that both the dynamical and equilibrium tide calculations give a power law with an index close to 4, which results in the circularization timescale being proportional to the binary period P_o to the 13/3. For comparison, Zahn (1977, 1989) and Goldman & Mazeh (1991), using equilibrium tide calculations, found t_{circ} to be proportional to P_o raised to the power 16/3, 13/3, and 10/3, respectively. The difference between these results can be related to a different choice of s in equation (13) for ν . These authors used an expression similar to equation (13) with, respectively, $s = 0, 1,$ and 2 . The fact that we obtain an index close to 13/3 by setting $s = 2$ or even 1 (see below), in contrast to the results above, is at least partially due to the effectively smaller value of c_2 that we used (see below).

We comment further that Tassoul (1988) found $t_{\text{circ}} \propto P_o^{49/12}$ for his postulated alternative hydrodynamical mechanism for tidal circularization.

3.3. Comparison between Calculations Based on the Dynamical and Equilibrium Tides

The results presented above show that the torque corresponding to the dynamical tide is smaller than that given by the adiabatic equilibrium tide for all of the frequencies that we have computed. However, the difference tends to decrease as the frequency gets smaller. From equations (36) and (37) we calculate that the ratio of these torques is indeed about 6.0 and 4.8 for $P_o = 4.23$ and 12.4 days, respectively.

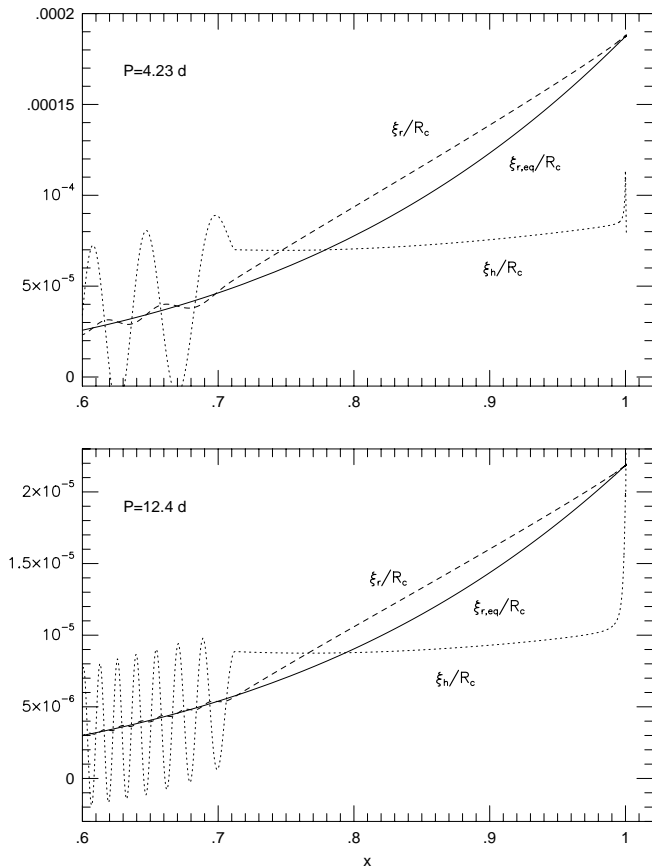


FIG. 3.— $\xi_{r,eq}/R_c = \xi_{h,eq}/R_c$ (solid line), ξ_r/R_c (dashed line), and ξ_h/R_c (dotted line) in units of $M_p/(M_p + M_\odot)$ vs. x for $0.6 \leq x \leq x_{out}$ and for $P_o = 4.23$ (top) and 12.4 (bottom) days.

Figure 3 shows $\xi_{r,eq}/R_c = \xi_{h,eq}/R_c$, ξ_r/R_c , and ξ_h/R_c in units of $M_p/(M_p + M_\odot)$ versus x in the range $0.6 \leq x \leq x_{out}$ for $P_o = 4.23$ and 12.4 days. It is clear from these plots that ξ_r and ξ_h depart from the asymptotic value in the convective envelope. The difference is not very large, but the derivatives of ξ_r and ξ_h from which the torque is calculated (see eq. [15]) depart more from their asymptotic values.

In the limit where the magnitude of the Brunt-Väisälä frequency is everywhere large compared to the tidal forcing frequency, calculations based on the dynamical tide should converge toward those based on the equilibrium tide. This is because the convective timescale is small enough that the convective motions adjust essentially instantaneously to the tidal forcing.

We have checked this expectation by artificially increasing the magnitude of the Brunt-Väisälä frequency in the convection zone. Except in the part of the convective envelope just below its outer radius, wherever $|N^2| < q\omega^2$, q being an arbitrary constant, we make the replacement $N^2 = -q\omega^2$. In Figure 4 we plot $\xi_{r,eq}/\xi_r$ versus x in the range $0.6 \leq x \leq x_{out}$ for $P_o = 12.4$ days and for $q = 10, 100$, and 400 . For comparison we also plot the case corresponding to the original solar model.

As expected, $\xi_{r,eq}/\xi_r$ converges toward 1 when the magnitude of the Brunt-Väisälä frequency is increased. We note that $q = 400$, which corresponds to $|N| \geq 10m\omega$, gives $1 - \xi_{r,eq}/\xi_r < 5\%$. This confirms that the asymptotic limit is reached when the magnitude of the Brunt-Väisälä frequency is very large compared to the frequency of the tidal wave.

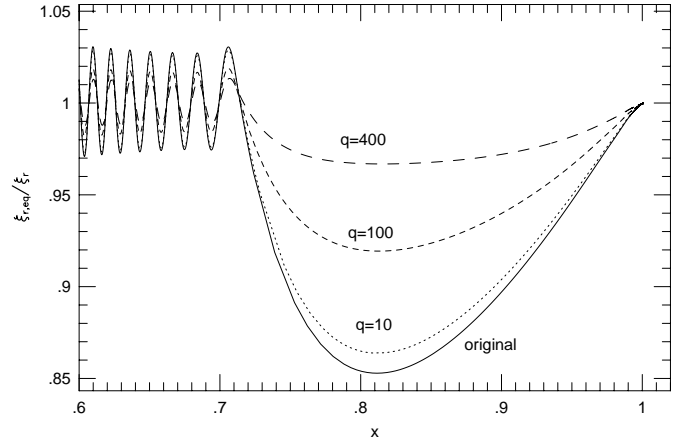


FIG. 4.— $\xi_{r,eq}/\xi_r$ vs. x in the range $0.6 \leq x \leq x_{out}$ for $P_o = 12.4$ days and for $q = 10$ (dotted line), 100 (short-dashed line), and 400 (long-dashed line), the definition of which is given in the text. For comparison we have also plotted the case corresponding to the original solar model (solid line). $\xi_{r,eq}/\xi_r$ is close to 1 when $|N| \gg m\omega$.

We note that the very slow convergence toward the equilibrium tide was predicted from the arguments presented in § 2.2. Also expected was the discontinuity in the mean value of ξ_h , obtained after averaging out the interior oscillations, at the boundary of the radiative core and the convection zone that is observed in Figure 3 (see also Fig. 1).

3.4. Calibration of the Turbulent Viscosity

We shall limit the comparison of our results with observations of main-sequence binaries because our calculations do not apply to pre-main-sequence stars, which have a much larger convective envelope than the Sun. As mentioned above, the observed circularization timescale we have to fit is then 4 Gyr for $P_o = 12.4$ days (Mathieu 1994). As indicated above, when using a simple estimate of the turbulent viscosity based on mixing-length theory for non-rotating stars, the circularization timescale we obtain from our calculations for this period is 56 times larger than 4 Gyr. This indicates either (i) that solar-type binaries are not circularized through turbulent viscosity acting on tidal perturbations (but see Tassoul 1988 and Kumar & Goodman 1996 for other suggested tidal mechanisms), or (ii) that dissipation in the convective envelope of solar-like stars is significantly more efficient than is currently estimated.

Tassoul (1995) postulates that efficient tidal dissipation occurs in a very thin Eckman layer close to the surface of a tidally deformed star and that this process greatly increases the efficiency of tidal interactions. But a refutation of the notion that the free surface boundary condition appropriate to the tidally deformed star, rather than the more common rigid boundary condition, leads to such an effective boundary layer has been given by Rieutord & Zahn (1997). Further Tassoul & Tassoul (1997) state that their mechanism is inapplicable to extreme mass ratio cases, such as 51 Pegasi, that we consider later in the paper.

We now consider briefly here the mechanism proposed by Kumar & Goodman (1996), namely enhanced dissipation associated with high-order oscillation modes excited through parametric instability. The growth rate for the most rapidly growing modes is expected to be $\sigma \sim m\omega\xi_r/R_\odot$, where ξ_r is the radial displacement in the primary

oscillation, which we shall assume to be the equilibrium tide, evaluated at $r = R_\odot$, and $m\omega$ is its frequency.

If we assume that the nonlinear development of the parametric instability and subsequent dissipation of the excited modes leads to an effective viscosity and frictional dissipation rate $t_f^{-1} = \sigma$, which is big enough to suppress the linear instability, then we expect from the classical theory of Darwin (1879) that there will be a phase lag θ_t associated with the tide given by

$$\theta_t = \sigma \frac{R_\odot^3}{GM_\odot} \omega. \quad (38)$$

For a binary of unit mass ratio and period ~ 10 days, synchronization occurs on a timescale very much shorter than that required for circularization, so that we assume that the stellar rotation is synchronized with the orbit and $m = 1$ in the calculation of σ . For small eccentricity, the circularization timescale t_{circ} is approximately given by $1/t_{\text{circ}} = \Omega_a \theta_t$, where the apsidal motion frequency is $\Omega_a = 15k(M_p/M_\odot)(R_\odot/D)^5\omega$, with k being the apsidal motion constant (Cowling 1938). We use the equilibrium tide value (eq. [30]) to estimate ζ_r/R_\odot at $r = R_\odot$ as $(R_\odot/D)^3/4$ for a mass ratio of unity. We then get $1/t_{\text{circ}} = 7.5k\omega(R_\odot/D)^{11} \propto \omega^{2.5/3}$ for θ_t given by equation (38). For an orbital period of 12.4 days, this gives $t_{\text{circ}} = 6 \times 10^3/k$ Gyr. Since $k \sim 0.01$, it is not very likely that this mechanism will be able to explain the observed circularization rates. However, we stress that this has not been shown from a full nonlinear calculation of the development of parametric instability.

3.4.1. Enhanced Turbulent Viscosity

In general, a large increase in the simply estimated turbulent viscosity coefficient is needed in order to explain the observed circularization rate. We now investigate what is needed to achieve this and give the numerical results of tests that we have carried out. In all cases, we have checked that *the velocity at the surface of the star is not sensitive to the magnitude of the turbulent viscosity assumed.*

In addition, as indicated above, the resonances are essentially controlled by radiative damping in the radiative core as long as $\gamma' \gg \gamma$. When the turbulent viscosity is enhanced, γ is increased. However, in the tests that we present below, for orbital periods larger than ~ 8 days, γ' stays large enough compared to γ so that although the nonresonant torques increase, the central structure and strength of the resonances is determined by radiative damping. For orbital periods on the order of ~ 4 days and $c_2 = 1$, γ can become comparable to γ' . Then the damping factor in equation (17) has to be replaced by $(\gamma + \gamma')^2$, and the strength of the resonance is reduced by a factor of ~ 4 .

We first consider the effect on the circularization timescale of varying the parameters c_1 , c_2 , s , and Λ in equation (13) for v . Note that the denominator we used in this expression is $1 + c_2(mt_c/P_o)^2$, rather than $1 + c_2(m\omega t_c)^2$. Using the latter with $c_2 = 1$ is equivalent to setting $c_2 = (2\pi)^2$ in the former. At present, it seems that our knowledge of convection does not allow discrimination between these possibilities (see, e.g., the discussion in Zahn 1989). However, we note that Goodman & Oh (1997) have recently put forward some arguments in favor of $c_2 = (2\pi)^2$. Using $c_2 = (2\pi)^2$ in equation (13) results in a circularization time for $P_o = 12.4$ days that is 10 times larger than that obtained with $c_2 = 1$. If we set $c_2 = 0$, t_{circ} is decreased by only a factor of 2. This is because when $c_2 = 1$, the factor

TABLE 2

t_{circ} FOR DIFFERENT VALUES OF s AND c_2

P_o (days)	c_2	s	t_{circ} (Gyr)
4.23.....	1	2	2.46
	...	1	1.37
12.4.....	...	2	220
	...	1	211
4.23.....	$(2\pi)^2$	2	39.4
	2π	1	5.98
12.4.....	$(2\pi)^2$	2	2010
	2π	1	685

$c_2(mt_c/P_o)^2$ is already smaller than (or even very small compared to) unity in a large part of the convective envelope. Thus it seems that adjusting the way in which turbulent viscosity responds to short period forcing cannot produce the required enhancement in this case.

In Table 2 we summarize the results obtained for different values of s and c_2 for the case of mass ratio unity, and in Table 3 we indicate the corresponding index of the power law in equation (37). We note that $c_2 = 1$ corresponds to the denominator in equation (13) being $1 + (mt_c/P_o)^s$, whereas $c_2 = (2\pi)^s$ corresponds to $1 + (m\omega t_c)^s$.

We note that setting $c_2 = (2\pi)^2$ with $s = 2$ decreases the index of the power law in equation (37) to ~ 3.3 . This gives a t_{circ} proportional to the orbital period to the $\sim 11/3$, which is similar to the value found by Goldman & Mazeh (1991).

Zahn & Bouchet (1989) have argued that the prescription $s = 2$ suggested by Goldreich & Keeley (1977) and used later by Campbell & Papaloizou (1983) and Goldman & Mazeh (1991; see also Goodman & Oh 1997) would lead to cutoff periods that are in clear conflict with the observational data, which they claim require $s = 1$. The results presented for the model adopted here do not support this statement. If $c_2 = 1$, t_{circ} hardly changes when s is changed from 2 to 1. If $c_2 = (2\pi)^s$, the difference between $s = 1$ and $s = 2$ is not dramatic for $P_o \sim 8$ –12 days. Within the uncertainties associated with convection, our results do not allow a distinction to be made between $s = 1$ and $s = 2$.

Finally, taking the mixing length to be the distance to the top boundary of the convective envelope rather than 3 times the pressure scale height does not significantly affect the circularization timescale.

We note that the torque is directly proportional to c_1 and α^2 . However, c_1 is expected to be on the order of unity, and α is usually taken to be between 1 and 4.

3.4.2. Modifications to the Brunt-Väisälä Frequency

The magnitude of the turbulent viscosity given by equation (13) would be increased if the magnitude of the Brunt-Väisälä frequency were larger in the convection zone.

TABLE 3

INDEX OF THE POWER LAW IN EQUATION (37) FOR DIFFERENT VALUES OF s AND c_2

c_2	s	Index of Power Law
1.....	2	3.85
	1	4.3
$(2\pi)^2$	2	3.3
2π	1	4.1

This is because the convective timescale decreases. We comment that a reduction in the convective timescale while the same length scale is maintained implies larger convective velocities that would have to occur without increasing the heat flux. This is the essential feature of the modification. To illustrate the effect of increasing the Brunt-Väisälä frequency, we consider the following dimensionless number:

$$\eta = \frac{N^2}{g} \left(\frac{d \ln P}{dr} \right)^{-1},$$

which is the superadiabatic temperature gradient when radiation pressure and variations of the mean molecular weight are neglected. The accuracy with which η is known from helioseismic observations is not better than $\sim 10^{-2}$ (Gough 1984). However, in most of the convective envelope, this parameter, estimated from mixing-length theory applied to nonrotating stars, is much smaller than 10^{-2} .

We have made a numerical investigation in which we increased $|N^2|$ in the convection zone by replacing η by $\min(p\eta, 10^{-3})$, p being an arbitrary constant, wherever $\eta \leq 10^{-3}$ (except just below the outer radius of the convective envelope). We have considered $p = 50$ and 100 . It is doubtful that consideration of present helioseismic data could preclude such an increase of $|N^2|$ (Thompson 1997).

Figure 5 shows η in the convective envelope versus x for

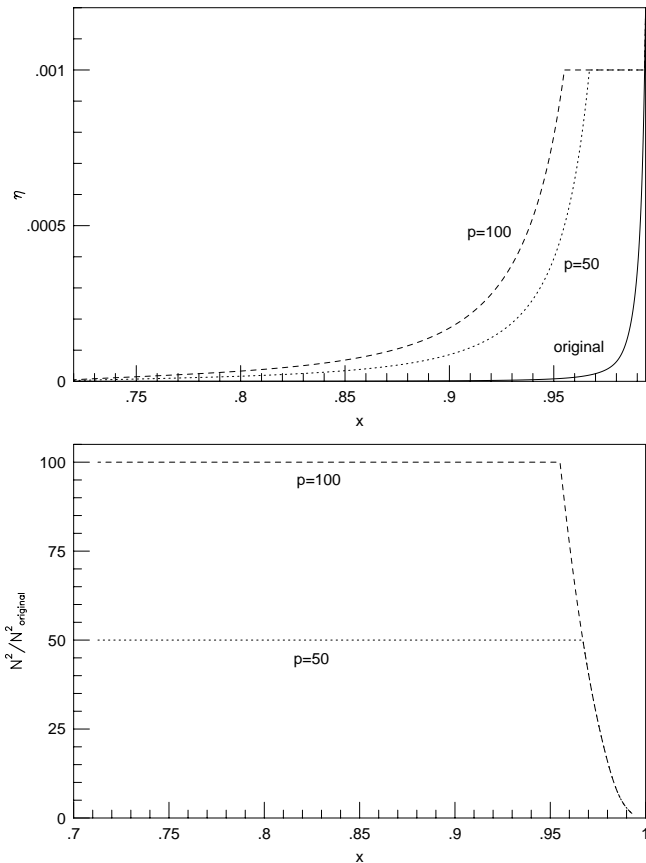


FIG. 5.—*Top*: Dimensionless parameter $\eta = N^2/(gd \ln P/dr)$ in the convective envelope vs. x . The curves correspond to the original solar model (solid line) and to the models with increased $|N^2|$ ($p = 50$ [dotted line] and 100 [dashed line], where p is as defined in the text). *Bottom panel*: Factor by which $|N^2|$ is increased in the convective envelope vs. x . N^2_{original} corresponds to the original solar model, and N^2 corresponds to the models with $p = 50$ (dotted line) and $p = 100$ (dashed line).

the original solar model and for $p = 50$ and $p = 100$. We also display the factor by which $|N^2|$ has been increased in each case.

The circularization timescales that we find with $c_2 = 1$ and $s = 2$ for $P_o = 12.4$ days when $p = 50$ and 100 are, respectively, 13 and 7.7 Gyr, which are now larger than the observed value by factors of 3 and 2, respectively. Small discrepancies of this magnitude could be dealt with by adjustments to the mixing length or c_1 . When either $p = 50$ or $p = 100$, the circular orbit torque is found to be proportional to $\omega^{4.6}$.

If, keeping $s = 2$, we adopt $c_2 = (2\pi)^2$, t_{circ} is increased only by a factor of 1.3 compared to the case of $c_2 = 1$ for $p = 100$. This is because the factor $c_2(mt_c/P_o)^2$ is smaller than (or even very small compared to) unity in almost all the convection zone, whatever the value of c_2 between 1 and $(2\pi)^2$.

Although an increase in $|N^2|$ of the magnitude that we consider might be thought to be unrealistic, we note that such an increase in the deep layers of the convection zone has also been considered by D'Silva (1995) as a means of explaining the dynamics of sunspots without invoking too strong a magnetic field. In his model, which applies strictly to a star rotating at the same rate as the sun, $|N^2|$ has to be larger than $4 \times 10^{-11} s^{-2}$, which means that it has to be multiplied on average by a factor of ~ 8 . In the solar model we use, we need to multiply $|N^2|$ by a factor of between 100 and 400 for $0.722 \geq x \geq 0.713$, between 10 and 100 for $0.828 \geq x \geq 0.722$, and between 1 and 10 for $0.915 \geq x \geq 0.828$ in order to obtain such a minimum value. If we do this, the circularization timescale that we obtain for $P_o = 12.4$ days is only 6 times larger than the observed one. In this context, it is possible that if the proposed increase in $|N^2|$ is related to the stellar rotation, this may be even greater for the more rapidly synchronously rotating star that is expected in the equal-mass binary case.

We note that numerical simulations of turbulent convection in the presence of rotation show an increase of $|N^2|$ with the effect of rotation (Brummell, Hurlburt, & Toomre 1996). This is because, as pointed out by Brummell et al. (1996), rotation influences the thermodynamic mixing properties of the convection in such a way that it leads to a decrease in correlation between temperature fluctuations and vertical velocities. The efficiency of the vertical convective transport is then weakened, with a subsequent enhanced superadiabatic mean stratification in the interior of the fluid (see their Fig. 8a). This suggests that the magnitude of the Brunt-Väisälä frequency in the convective envelope of rotating stars is actually larger than the values given by the solar model that we have been using here. However, it seems questionable that the extremely large increase required to account for the observed circularization rates can be achieved.

3.4.3. Turbulent Viscosity below the Convection Zone

Another means of increasing the total amount of dissipation is to assume that turbulent viscosity acts down to some depth below the inner boundary of the convective envelope. This might be expected if convective overshooting takes place. However, this might not be a very effective process because of the slow convective motions expected and the rapid increase in $|N^2|$ that occurs as the radiative zone is entered.

Estimates based on the observed solar oscillation frequencies give an upper limit of between 0.05 (Basu 1997) and ~ 0.1 (Christensen-Dalsgaard, Monteiro & Thompson 1995) times the pressure scale height on the extent of overshoot below the convection zone.

Here we consider a simple illustrative situation in which convective blobs or some other turbulent motions are able to penetrate into the stratified radiative core over some fraction z of the pressure scale height $|d \ln P/dr|^{-1}$, producing a turbulent viscosity. We model this by setting ν to be constant from a distance $0.5z|d \ln P/dr|^{-1}$ above the inner radius of the convective envelope down to the same distance below this radius, equal to its value at the top of this zone. Because such a viscosity is able to act on the short-wavelength part of the tidal response associated with g -modes, it has a dramatic effect.

For $z = 1$ and $c_1 = c_2 = 1$, the circularization timescale for $P_o = 12.4$ days is decreased by a factor of about 400, being now 8 times smaller than the observed timescale. If we set $c_2 = (2\pi)^2$ (see discussion above), t_{circ} is increased by a factor of 15, being about 4 times larger than the observed timescale.

For $z = 0.1$ and $c_1 = c_2 = 1$, we get a circularization timescale for $P_o = 12.4$ days that is about 30 times larger than that observed. For the calculated timescale to be in agreement with the observations, we need z to be between 0.4 and 0.5, with $c_1 = c_2 = 1$. In the model that we have adopted, the effect is of less importance for shorter periods, because the number of oscillations of the response in the region of the radiative core where turbulent dissipation is introduced decreases with forcing frequency. Therefore, the torque does not vary with ω as a simple power law with an index close to 4. However, in reality, the effectiveness of the turbulent viscosity should be reduced for short wavelength disturbances, giving a compensating effect to make it relatively less effective at low frequencies.

The above calculations show that overshooting is not likely to be efficient enough to decrease the circularization timescales by a factor of about 50. To get such an effect, we indeed require an extent of overshoot below the convection zone that is at least 5 or 10 times larger than that deduced from the observations. In addition, we have not taken into account the fact that overshooting leads to an increase of the g -modes length scale through a decrease in the buoyancy or the magnitude of N^2 . This in turn would decrease the amount of turbulent dissipation associated with overshooting.

3.5. Fitting the Observations

As we have already mentioned above, *calculations based on both the dynamical and equilibrium tide theories give a torque that is proportional to the orbital frequency raised to a power of ~ 4* (see eqs. [36] and [37]). If circularization of solar-type binaries does occur through the action of turbulent viscosity on the tides, then its magnitude has to be calibrated so as to account for the observed timescale. We have discussed in § 3.4, somewhat speculatively, how the required enhancement of the magnitude of the viscosity above that obtained from simple estimates might be envisaged to occur. Since the enhancement might depend on forcing frequency, it is not clear that the resulting torque will still be proportional to the frequency to a power of ~ 4 . However, the increase to $|N^2|$ described above gave torques

that approximately preserved this power law, so that in the absence of additional information, we shall suppose that it holds. Then the calibration acts only to adjust the coefficient of the power law.

We note that the observations do not rule out any exponent between 3 and 5 (see below). Since our calculations can only strictly be applied to solar-type stars, we calibrate our results using $t_{\text{circ}} = 4$ Gyr for $P_o = 12.4$ days. This gives (in cgs)

$$\mathcal{T}(\text{g cm}^2 \text{ s}^{-2}) = 5.086 \times 10^{35} \left(\frac{M_p}{M_p + M_\odot} \right)^2 \left(\frac{\omega}{10^{-5} \text{ s}^{-1}} \right)^4, \quad (39)$$

or, equivalently,

$$\mathcal{T}(\text{g cm}^2 \text{ s}^{-2}) = 1.423 \times 10^{39} \left(\frac{M_p}{M_p + M_\odot} \right)^2 \left(\frac{P_o}{1 \text{ day}} \right)^{-4}. \quad (40)$$

The corresponding formulæ for the orbital and spin-up timescales (in Gyr) are

$$t_{\text{orb}}(\text{Gyr}) = 2.763 \times 10^{-4} \frac{(M_p/M_\odot + 1)^{5/3}}{M_p/M_\odot} \left(\frac{P_o}{1 \text{ day}} \right)^{13/3}, \quad (41)$$

$$t_{\text{sp}}(\text{Gyr}) = 1.725 \times 10^{-6} \left(\frac{M_p + M_\odot}{M_p} \right)^2 \left(\frac{P_o}{1 \text{ day}} \right)^3, \quad (42)$$

and $t_{\text{sp},c} = I_c t_{\text{sp}}/I$ (for the solar model that we use, $I = 1.064 \times 10^{54}$ and $I_c = 1.5 \times 10^{53} \text{ g cm}^2$).

Since the torque is proportional to ω^4 , we can use equation (35) for t_{circ} , so that the circularization time is given by

$$t_{\text{circ}}(\text{Gyr}) = 4.605 \times 10^{-5} \frac{(M_p/M_\odot + 1)^{2/3}}{M_p/M_\odot} \left(\frac{P_o}{1 \text{ day}} \right)^{13/3}. \quad (43)$$

Even though our calculations can only be applied to solar-type stars, it is of interest to compare the circularization timescales that we obtain from equation (43) to the observed ones. For $P_o = 4.3, 7.05, 8.5,$ and 18.7 days, equation (43) gives, respectively, $t_{\text{circ}} = 0.04, 0.3, 0.8,$ and 24 Gyr, to be compared to the observed timescales of $0.003, 0.1, 0.8,$ and 16 Gyr, respectively. The agreement for $P_o \geq 8.5$ days is within a factor of 1.5. For smaller periods, circularization is expected to occur when the convective envelopes of the stars are larger, making turbulent dissipation more efficient. We note that Mathieu et al. (1992) have already pointed out that a power law $t_{\text{circ}} \propto P_o^{13/3}$ provides a close fit to the slope of the observed cutoff periods. However, the observations are equally well fitted with an index of $10/3$, and an index of $16/3$ cannot be ruled out (Mathieu et al. 1992).

If the simple estimate of the turbulent viscosity based on mixing-length theory for nonrotating stars is used, the coefficients in the formulæ for the torque have to be divided by a factor of ~ 50 , whereas those in the formulæ for the timescales have to be multiplied by the same factor.

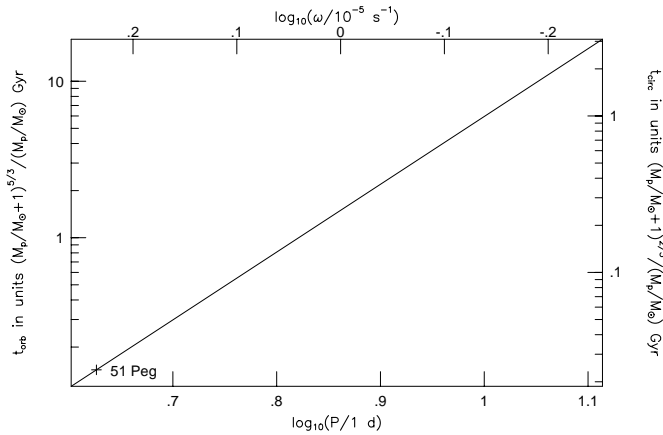


FIG. 6.—Graph of t_{orb} in units $(M_p/M_\odot + 1)^{5/3}/(M_p/M_\odot)$ Gyr (eq. [41]) and t_{circ} in units $(M_p/M_\odot + 1)^{2/3}/(M_p/M_\odot)$ Gyr (eq. [43]) vs. ω and P in a log-log representation. The cross indicates the position of 51 Pegasi. These timescales fit the observations. If instead they are calculated using the simple estimate of the turbulent viscosity based on mixing-length theory, they have to be multiplied by ~ 50 .

In Figure 6 we have plotted t_{orb} in units of $(M_p/M_\odot + 1)^{5/3}/(M_p/M_\odot)$ and t_{circ} in units of $(M_p/M_\odot + 1)^{2/3}/(M_p/M_\odot)$ versus ω and P_o in a log-log representation.

4. DISCUSSION

4.1. Application to 51 Pegasi

It is of interest to apply these results to the system 51 Pegasi, for which the orbital period (assuming that the observed oscillations are caused by a companion) is $P_o = 4.23$ days. If the companion is a Jupiter mass planet ($M_p = 10^{-3} M_\odot$), then the tidal orbital evolution timescale given by equation (41) is $t_{\text{orb}} \sim 140$ Gyr, the star spin-up timescale (eq. [42]) is $t_{\text{sp}} \sim 130$ Gyr, and the spin-up timescale of the convective envelope is $t_{\text{sp,c}} \sim 18$ Gyr. All of these timescales are long compared to the inferred age of 51 Pegasi (Edvardsson et al. 1993). If the companion is a low-mass star of $0.1 M_\odot$, as has been recently suggested, t_{orb} is 100 times smaller, while t_{sp} and $t_{\text{sp,c}}$ are 10^4 times smaller. We then expect the primary star to be synchronized with the orbit, in which case exchange of angular momentum is no longer taking place. Synchronization is actually expected if the mass of the companion is larger than about 10 Jupiter masses. The orbital decay timescale is also smaller than the age of the system, but since $t_{\text{sp}} < t_{\text{orb}}$, tidal interaction stops before the companion has plunged into the central star.

If the simple estimate of the turbulent viscosity based on mixing-length theory for nonrotating stars is used, all these timescales have to be multiplied by ~ 50 . In that case synchronization is expected if the mass of the companion is larger than about 70 Jupiter masses.

The planetary companion interpretation has been questioned recently by the reported 4.23 day modulation in the line profile of 51 Pegasi (Gray 1997), and the possibility that this modulation may be caused by g -mode oscillations has been considered (Gray & Hatzes 1997).

We note that, according to our results, such a modulation could not arise from g -mode oscillations tidally driven by a companion. For the oscillation to have a period of 4.23 days, the orbital period would have to be 8.46 days. The

maximum perturbed radial velocity induced by the companion at the surface of the star would then be between 2×10^{-3} and 1 m s^{-1} for a perturbing mass of between 10^{-3} and $1 M_\odot$. These numbers do not depend on the magnitude of the turbulent viscosity assumed, and they are not expected to be affected by the possibility of resonance. These velocities are at least about 50 times smaller than those observed.

4.2. Summary

In this paper we have studied the dynamical response of a star to the tidal perturbation of a companion. We have computed the torque caused by dissipation in the convective envelope using first-order perturbation theory. In the vicinity of resonance, we have also calculated the torque arising from nonadiabaticity in the radiative core using a WKB treatment. We have found that the torque at effective resonances is mainly determined by radiative damping. We have carried out an analysis based on the adiabatic equilibrium tide and showed that agreement with the dynamical tide calculations can be rather poor. For the unmodified stellar model and the periods of interest of several days, the torque derived using the equilibrium tide is 4–6 times larger than that corresponding to the dynamical tide.

We have found that the presence of fixed resonances does not affect the long-term orbital evolution of the binary, so that the different timescales (orbital evolution, circularization, and spin-up) are mainly determined by the nonresonant interaction. Our calculations show that the viscosity that is required to provide the observed circularization rates of solar-type binaries is ~ 50 times larger than that simply estimated from mixing-length theory for nonrotating stars.

We have explored some means by which this viscosity might be enhanced. We have found that it could become large enough if the magnitude of the Brunt-Väisälä frequency in the deep convective envelope were increased sufficiently. Such an increase is expected to be produced by the effect of rotation on convection, but it is questionable whether it can be of sufficient magnitude.

We note that the strength of the resonances for orbital periods larger than ~ 8 days and the perturbed velocity at the surface of the star are insensitive to the magnitude of the turbulent viscosity assumed. Only for periods of ~ 4 days and $c_2 = 1$ is the strength of the resonances decreased by a factor of ~ 4 . The effective widths of the resonances affecting the tidal torques are also reduced when the viscosity is increased.

We have applied our results to 51 Pegasi and showed that the oscillations that have been observed at the surface of this star cannot be a tidally driven nonradial g -mode. Also, we have found that the stellar rotation and the orbital motion of this system are expected to be synchronized if the mass of the companion exceeds $0.1 M_\odot$.

We are grateful to M. J. Thompson for supplying us with a solar model, and we thank D. O. Gough, R. D. Mathieu, and M. J. Thompson for helpful discussions. This work is supported by PPARC through grant GR/H/09454 and by NSF and NASA through grants AST 93-15578 and NAG 5-4277. C. T. and D. N. C. L. acknowledge support by the Center for Star Formation Studies at NASA/Ames Research Center and the University of California at Berkeley and Santa Cruz.

REFERENCES

- Basu, S. 1997, *MNRAS*, 288, 572
 Brummell, N. H., Hurlburt, N. E., & Toomre, J. 1996, *ApJ*, 473, 494
 Campbell, C. G., & Papaloizou, J. C. B. 1983, *MNRAS*, 204, 433
 Christensen-Dalsgaard, J., & Berthomieu, G. 1991, in *Solar Interior and Atmosphere*, ed. A. N. Cox, W. C. Livingston, & M. S. Matthews (Tucson: Univ. Arizona Press), 401
 Christensen-Dalsgaard, J., et al. 1996, *Science*, 272, 1286
 Christensen-Dalsgaard, J., Monteiro, M. J. P. F. G., & Thompson, M. J. 1995, *MNRAS*, 276, 283
 Claret, A., & Cunha, N. C. S. 1997, *A&A*, 318, 187
 Cowling, T. G. 1938, *MNRAS*, 98, 734
 ———. 1941, *MNRAS*, 101, 367
 Darwin, G. H. 1879, *Phil. Trans. Roy. Soc.*, 170, 1
 D'Silva, S. 1995, *ApJ*, 443, 444
 Edvardsson, B., Anderson, J., Gustafsson, B., Lambert, D. L., Nissen, P. E., & Tomkin, J. 1993, *A&A*, 275, 101
 Goldman, I., & Mazeh, T. 1991, *ApJ*, 376, 260
 Goldreich, P., & Keeley, D. A. 1977, *ApJ*, 211, 934
 Goldreich, P., & Nicholson, P. D. 1989, *ApJ*, 342, 1079
 Goldstein, H. 1980, *Classical Mechanics* (2d ed.; Cambridge, MA: Addison-Wesley), 267
 Goodman, J., & Oh, S. P. 1997, *ApJ*, 486, 403
 Gough, D. O. 1984, *Mem. Soc. Astron. Italiana*, 55, 13
 Gray, D. F. 1997, *Nature*, 385, 795
 Gray, D. F., & Hatzes, A. P. 1997, *ApJ*, 490, 412
 Kumar, P., & Goodman, J. 1996, *ApJ*, 466, 946
 Marcy, G. W., & Butler, R. P. 1995, *IAU Circ.* 6251
 Marcy, G. W., Butler, R. P., Williams, E., Bildsten, L., Graham, J. R., Ghez, A. M., & Jernigan, J. G. 1997, *ApJ*, 481, 926
 Mathieu, R. D. 1992, in *Binaries as Tracers of Stellar Formation*, ed. A. Duquennoy & M. Mayor (Cambridge: Cambridge Univ. Press), 155
 ———. 1994, *ARA&A*, 32, 465
 Mathieu, R. D., Duquennoy, A., Latham, D. W., Mayor, M., Mazeh, T., & Mermilliod, J.-C. 1992, in *Binaries as Tracers of Stellar Formation*, ed. A. Duquennoy & M. Mayor (Cambridge: Cambridge Univ. Press), 278
 Mathieu, R. D., & Mazeh, T. 1988, *ApJ*, 326, 256
 Mayor, M., & Mermilliod, J.-C. 1984, in *IAU Symp. 105, Observational Tests of Stellar Evolution Theory*, ed. A. Maeder & A. Renzini (Dordrecht: Reidel), 411
 Mayor, M., & Queloz, D. 1995, *Nature*, 378, 355
 Papaloizou, J. C. B., & Savonije, G. J. 1985, *MNRAS*, 213, 85
 ———. 1997, *MNRAS*, 291, 651
 Press, W. H., Flannery, B. P., Teukolsky, S. A., & Vetterling, W. T. 1986, *Numerical Recipes: The Art of Scientific Computing* (2d ed.; Cambridge: Cambridge Univ. Press)
 Rasio, F. A., Tout, C. A., Lubow, S. H., & Livio, M. 1996, *ApJ*, 470, 1187
 Rieutord, M., & Zahn, J. P. 1997, *ApJ*, 474, 760
 Savonije, G. J., & Papaloizou, J. C. B. 1983, *MNRAS*, 203, 581
 ———. 1984, *MNRAS*, 207, 685
 ———. 1997, *MNRAS*, 291, 633
 Savonije, G. J., Papaloizou, J. C. B., & Alberts, F. 1995, *MNRAS*, 277, 471
 Tassoul, J.-L. 1988, *ApJ*, 324, L71
 ———. 1995, *ApJ*, 444, 338
 Tassoul, M., & Tassoul, J.-L. 1997, *ApJ*, 481, 363
 Thompson, M. J. 1997, private communication
 Unno, W., Osaki, Y., Ando, H., Saio, H., & Shibahashi, H. 1989, *Nonradial Oscillations of Stars* (2d ed.; Tokyo: Univ. Tokyo Press)
 Xiong, D. R., Cheng, Q. L., & Deng, L. 1997, *ApJS*, 108, 529
 Zahn, J. P. 1966, *A&A*, 29, 489
 ———. 1975, *A&A*, 41, 320
 ———. 1977, *A&A*, 57, 383
 ———. 1989, *A&A*, 220, 112
 Zahn, J. P., & Bouchet, L. 1989, *A&A*, 223, 112

Note added in proof.—At the proof stage we became aware of a paper submitted by J. Goodman and E. S. Dickson on tides in a solar-type star. These authors adopted a smaller estimate of the turbulent viscosity, equivalent to $c_2 = (2\pi)^2$, than in this paper. Their results then indicate that torques due to nonadiabatic effects become comparable to those caused by turbulent viscosity at periods of about 5 days midway between resonances. This is consistent with our results quoted in § 3.2.2.1 if the value $c_2 = (2\pi)^2$ is used (see Table 2).